

support for this assignment, and the value of four for N is thus understood, for example, as the Ag^+ is more or less completely surrounded by solvent molecules and thus "solvent shielded" from the NO_3^- ion. The 1036-cm^{-1} line which is observed at higher concentrations is assigned to NO_3^- ions in a different force field, *i.e.*, perturbed in some way by the cations. The increase in the intensity of 1036-cm^{-1} line compared to that of the 1041-cm^{-1} line as the solute concentration is increased is understood as due to the direct interactions of the NO_3^- ions with cations. Penetration of the primary solvation sphere, with the displacement of a solvent molecule by the NO_3^- ion, leading to the formation of a contact ion pair (or inner-sphere complex), as suggested elsewhere,^{1,15} would be the equivalent of second type of NO_3^- species in these solutions. The presence of two kinds of NO_3^- ions for solutions of concentrations above 3 mol/l. is evident from the observation of the asymmetric shape of the band at $\sim 1039\text{ cm}^{-1}$.

The value α , the fraction of free NO_3^- ions in the solution, for concentrations less than ~ 0.5 mol/l., was calculated from the integrated intensity values of the 1036- and 1041-cm^{-1} bands, and the results are shown in Table II, together with the values of α calculated from the Wishaw-Stokes conductance equation¹⁶ and earlier conductance studies.¹⁷ The agree-

(16) B. F. Wishaw and R. H. Stokes, *J. Amer. Chem. Soc.*, **76**, 2065 (1954).

Table II. α , the Fraction of Free NO_3^- Ions in $\text{AgNO}_3\text{-CH}_3\text{CN}$ Solutions

Concentration, M	0.03	0.05	0.1	0.2	0.25	0.50
α_{Raman}	0.72	0.63	0.56	0.48	0.46	0.44
$\alpha_{\text{conductance}}$	0.64	0.59	0.51	0.44	0.43	0.42

ment between the α values calculated from two different methods suggests that a study of the region of the most intense band of NO_3^- ion species, *i.e.*, the 1050-cm^{-1} region, opens the way to spectroscopic investigations of ion-ion association in the dilute solution region, *i.e.*, in a concentration range where spectroscopic and conductance approaches can be interfaced and in which the concepts of interionic attraction theory of electrolytes are still applicable. This has hitherto been denied, since the previously established criteria, *i.e.*, the 750- and $1300\text{-}1500\text{-cm}^{-1}$ regions, are the regions of weaker activity so that measurements at high dilutions are virtually impossible.

Acknowledgments. This work was made possible, in large part, by support received from the National Science Foundation and the U. S. Department of Interior, Office of Saline Water. Dr. Barry G. Oliver is thanked for the calculations of α from the electrical conductance data and helpful discussions.

(17) G. J. Janz, A. E. Marcinkowsky, and I. Ahmed, *J. Electrochem. Soc.*, **112**, 104 (1965).

Nature of Solvent Effects on the Proton Chemical Shifts of Nonpolar Solutes¹

Edmund R. Malinowski and Paul H. Weiner

*Contribution from the Department of Chemistry and Chemical Engineering,
Stevens Institute of Technology, Hoboken, New Jersey 07030.*

Received January 10, 1970

Abstract: Chemical shifts of nonpolar solutes in various solvents are referenced relative to external hexamethyl-disiloxane by utilizing a spinning coaxial sample technique. From a graphical analysis, values for the various factors which contribute to the solvent shifts are deduced. Values for van der Waals terms agree quantitatively with the binary collision model of Bernstein. Solvent anisotropy contributions for benzene and carbon disulfide are compared with the theoretical estimations of Schug. Furthermore, gas-phase shifts of nonpolar molecules are predicted from the graphs.

Most nmr studies are conducted on compounds dissolved in some solvent. It is well known that each solvent perturbs the chemical shift of a solute differently. Recently, Laszlo and coworkers² have shown qualitatively that the proton shifts of internal standards (such as tetramethylsilane, cyclohexane, and other nonpolar molecules) are affected dramatically by different solvents. However, quantitative examination of the data were not ventured by these authors since they them-

selves employed internal standards only. In order to study these systems in more detail we referenced the data of Laszlo² to an external standard basis, utilizing spinning coaxial sample techniques described herein. Additional solvents and nonpolar solutes were added to the scheme in order to broaden the study.

Experimental Section

Proton spectra were recorded with a Varian A60-A spectrometer operating at a probe temperature of $39 \pm 1^\circ$. The spectra were calibrated using a Hewlett-Packard Model 200AB wide range oscillator and a Hewlett-Packard Model 523DR frequency counter. All compounds were used as obtained from commercial sources. When possible, solvents were stored over molecular sieves. Samples were prepared by adding a trace of each solute to the sol-

(1) Presented at Metro Chem 69, Regional Meeting of the New York and North Jersey Sections of the American Chemical Society, New York, N. Y.

(2) P. Laszlo, A. Apeert, R. Ottinger, and J. Reisse, *J. Chem. Phys.*, **48**, 1732 (1968).

Table I. Chemical Shifts for TMS and CH₄ as Solutes *vs.* External Hexamethyldisiloxane^a

Solvent	$\delta_{\text{solV TMS},i}^b$	$\delta_{\text{solV HMD},x}^c$	$\delta_{\text{TMS HMD},x}^d$	$\delta_{\text{CH}_4 \text{TMS},i}^e$	$\delta_{\text{CH}_4 \text{HMD},x}^f$
CH ₃ CN	-117.6	-119.3	-1.7, ^g -1.8 ^h	-12.1	-13.9
(CH ₃) ₂ C=O	-125.0	-116.0	+9.0, ^g +8.8 ^h	-10.0	-1.1
CH ₃ I	-131.0	-136.8	-5.8, ^g -5.0 ^h	-12.9	-18.3
CH ₂ I ₂	-235.8	-255.0	-20.0, ^g -19.7 ^h	-15.1	-34.9
CH ₂ Br ₂	-300.8	-307.3	-6.5, ^g -7.0 ^h	-13.8	-20.6
CHBr ₃	-411.0	-422.1	-11.0, ^g -10.6 ^h	-15.2	-26.1
CH ₂ Cl ₂	-319.8	-318.6	+1.2, ^g +1.6 ^h	-12.1	-10.7
CHCl ₃	-436.1	-437.6	-1.9, ^h -1.9 ^h	-12.7	-14.6
CCl ₄			-2.8, ⁱ -3.1 ^h	-13.8	-16.8
CS ₂			-11.0, ⁱ -10.9 ^h	-13.3	-24.3
(CH ₃) ₂ S=O	-152.4	-158.5	-6.1, ^g -4.5 ^h	-19.9	-25.2
C ₆ H ₆	-429.7	-402.1	-27.6, ^g -26.5 ^h	-7.7	+19.3
C ₆ H ₁₂	-86.6	-84.1	+2.5, ^g +2.6 ^h	-11.1	-8.5
C ₆ H ₁₀	-90.8	-87.1	+3.7, ^g +4.0 ^h	-10.5	-6.8

^a All values in Hz at 60 MHz. Negative shifts indicate low-field shifts from the standard peaks. ^b Chemical shifts between solvent peaks and internal TMS. ^c Corrected shifts between external HMD and solvent peaks. ^d Corrected shifts between external HMD and internal TMS. ^e Chemical shifts between dissolved methane and internal TMS. ^f Corrected shifts between external HMD and dissolved methane. ^g Chemical shift value calculated from data in first two columns. ^h Chemical shifts calculated directly from coaxial tubes in which HMD was the standard and TMS was dissolved in the solvent. ⁱ Since no solvent peak is present, these values were calculated by using a different reference material than HMD and then correcting for the shift difference between the two reference standards.

vent, which also contained a trace amount of tetramethylsilane (TMS) as an internal reference standard.

To correct the internal standard work to an external reference basis, the chemical shift between internal TMS and external hexamethyldisiloxane (HMD) was determined using a coaxial sample cell. Bulk susceptibilities, needed to correct the chemical shifts, were measured accurately at 39° by a spinning coaxial cell method.

Bulk Susceptibility Corrections. When external standards are utilized, corrections must be made for the differences in bulk susceptibilities between the reference standard, $\chi_{v,\text{ref}}$, and the sample solution, $\chi_{v,\text{soln}}$. For cylindrical samples

$$\delta_{\text{cor}} = \delta_{\text{obsd}} - \frac{2\pi}{3}(\chi_{v,\text{soln}} - \chi_{v,\text{ref}}) \quad (1)$$

Here δ_{cor} is the corrected chemical shift and δ_{obsd} is the observed chemical shift. Bulk susceptibility corrections were obtained with the nmr spectrometer by utilizing spinning coaxial cells.^{3,4} The bulk susceptibilities were determined by two methods to check the accuracy of the technique. One method entailed the measuring of the splitting of the peak of the material in the annular region of a coaxial cell, when the reference was annular and the solution central and *vice versa*. One can show that

$$\chi_{v,\text{soln}} - \chi_{v,\text{ref}} = \frac{[\nu_s^{(1)} - \nu_s^{(2)}]kr^2}{(a^2 + b^2)\pi\nu_0} \quad (2)$$

Here $\nu_s^{(1)}$ is the spinning frequency when the reference is annular and the solution is central, $\nu_s^{(2)}$ is the spinning frequency when the sample is annular and the reference central, a and b are the inner and outer radii of the central tube, r is the mean radius of the annular region, k is the argument of the Bessel function relationship relating relative heights of the peak of the annular region to its first side band,³ and ν_0 is the spectrometer frequency. The argument k equals 1.4347 under the conditions when the first spinning side band is made equal in intensity to the main band.

The second method involved observing the spinning side bands of the reference in the annular region, with nitrogen gas, under 1 atm of pressure, in the central cell, and again with the solution in the central cell. Under these conditions

$$\chi_{v,\text{center}} \approx \chi_{v,\text{center}} - \chi_{\text{N}_2} = \frac{[\nu_s^{(1)} - \nu_s^{(3)}]kr^2}{(a^2 + b^2)\pi\nu_0} \quad (3)$$

Here $\nu_s^{(3)}$ is the splitting measured with the reference annular and nitrogen gas central. For both methods, the absolute sign of all $\nu_s^{(i)}$ were determined by the field-gradient method developed by Malinowski and Pierpaoli.⁴ By these procedures we estimate that

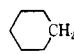
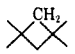
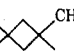
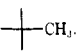
bulk susceptibilities can be measured within ± 0.005 cgs unit or better. The accuracy of the corrected chemical shifts is approximately ± 1.5 Hz or better.

Shift Measurements. The chemical shift between external HMD and internal TMS was obtained by two methods for comparison. The first method consisted of placing a trace amount of TMS in each solvent and then directly measuring its chemical shift relative to external HMD and applying the appropriate bulk susceptibility corrections. The second method employed the measuring of the chemical shift between internal TMS and the solvent peak, and, in a separate experiment, measuring the chemical shift between external HMD and the same solvent peak. From these two quantities, it was possible to obtain the chemical shifts between external HMD and internal TMS. Data for both methods are shown in Table I. All data were then referenced to an external basis by applying the correction factors listed in Table I.

Discussion

In Figure 1 the chemical shifts of various nonpolar solutes are plotted against the shifts of methane in the same solvent, with external HMD as the reference standard. Data used in this figure are found in Table II. The plots are linear, provided that benzene and

Table II. Chemical Shifts^a of Nonpolar Solutes Corrected to External HMD Standard

Solvent	Si(CH ₃) ₄					CH ₄
	b	c	c	c	c	b
CCl ₄	-3.0	-88.8	-78.5	-61.8	-58.6	-16.8
CS ₂	-11.0	-96.1	-85.2	-68.1	-65.6	-24.3
CDCl ₃	-1.9	-87.7	-77.9	-60.5	-57.1	-14.6
CH ₂ Cl ₂	+1.4	-84.8	-75.2	-57.3	-53.6	-10.7
Me ₂ CO	+8.9	-76.7	-68.9	-50.3	-46.6	-1.1
MeCN	-1.8	-87.9	-78.9	-60.9	-57.3	-13.9
Me ₂ SO	-5.0	-89.4	-79.9	-62.6	-59.4	-25.2
C ₆ H ₆	+27.0	-57.3	-47.8	-31.6	-27.3	+19.3
CH ₂ I ₂	-19.8	-98.6 ^b				-34.9
CH ₃ I	-5.4					-18.3
CH ₂ Br ₂	-6.7					-20.6
CHBr ₃	-10.8	90.7 ^b				-26.1
C ₆ H ₁₂	+2.5					-8.5
C ₆ H ₁₀	+3.8					-6.8


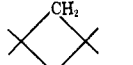
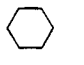
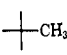
^a In Hz, negative values indicate low-field shifts. ^b Measured in this laboratory. ^c Data of P. Laszlo, A. Speert, R. Ottinger, and J. Reisse, *J. Chem. Phys.*, **48**, 1732 (1968), corrected to external HMD standard.

(3) R. F. Spanier, T. Vladimiroff, and E. R. Malinowski, *J. Chem. Phys.*, **45**, 4355 (1966).

(4) E. R. Malinowski and A. R. Pierpaoli, *J. Magn. Resonance*, **1**, 509 (1969).

carbon disulfide solvents are excluded from consideration. Reasons for this exclusion will be discussed later. Slopes and intercepts, calculated by a method of least squares, are given in Table III. Interestingly, the gas-

Table III. Least-Squares Slopes and Intercepts for Nonpolar Solutes^a

x axis	y axis	Slope	Intercept
Methane		0.75	-49.5
Methane		0.56	-69.4
Methane		0.56	-79.4
Methane	TMS	0.86	10.9
Methane		0.83	-44.8

^a Least-squares slopes calculated using the data for the halogenated solvents only.

phase shifts (TMS *vs.* methane and cyclohexane *vs.* methane) fall on these lines.

To understand the nature of these curves we refer to the work of Buckingham, Schaefer, and Schneider,⁵ who postulate that the screening constant of a solute molecule *i* in a solvent α is a linear sum of terms

$$\sigma(i, \alpha) = \sigma_g(i) + \sigma_b(\alpha) + \sigma_a(\alpha) + \sigma_w(i, \alpha) + \sigma_E(i, \alpha) \quad (4)$$

In this equation $\sigma_g(i)$ is the screening constant of solute *i* in the gas phase, $\sigma_b(\alpha)$ is the bulk susceptibility effect of solvent α , $\sigma_a(\alpha)$ is the anisotropy of the solvent, $\sigma_w(i, \alpha)$ is due to van der Waals dispersion interaction between solute *i* and solvent α , and $\sigma_E(i, \alpha)$ is the reaction field interaction between solute and solvent.

If an external standard is used and corrections are made for bulk susceptibility then the chemical shift is given by the expression

$$\delta_{\text{cor}}^{\text{ref}}(i, \alpha) = \delta_g^{\text{ref}}(i) + \sigma_a(\alpha) + \sigma_w(i, \alpha) + \sigma_E(i, \alpha) \quad (5)$$

where $\delta_g^{\text{ref}}(i) = \sigma(i) - \sigma_g(\text{ref})$, *i.e.*, the gas-phase shift of solute *i* relative to some reference standard.

For a nonpolar solute, which possess no net dipole moment, the reaction field term $\sigma_E(i, \alpha)$ is usually small and will be set equal to zero. Therefore the data plotted in Figure 1, the shifts of nonpolar solutes, referenced relative to external HMD and corrected for bulk susceptibility, can be expressed as

$$\delta_{\text{cor}}^{\text{HMD}, x}(i, \alpha) = \delta_g^{\text{HMD}}(i) + \sigma_a(\alpha) + \sigma_w(i, \alpha) \quad (6)$$

The fact that the gas-phase shifts fall on the line is predicted by eq 6. Since both $\sigma_a(\alpha)$ and $\sigma_w(i, \alpha)$ are small for gases at low pressures, then $\delta_{\text{cor}}^{\text{HMD}, x}(i, \alpha) = \delta_g^{\text{HMD}}(i)$. These graphs then provide us with a simple means of predicting gas-phase shifts from solution measurements. From Figure 1 we predict that the gas-phase shift relative to external HMD for neopentane is -40.5 Hz; for the methyl group of 1,1,3,3-tetramethylcyclobutane, -44 Hz; for the methylene group of 1,1,3,3-

(5) A. D. Buckingham, T. Schaefer, and W. G. Schneider, *J. Chem. Phys.*, **32**, 1227 (1960).

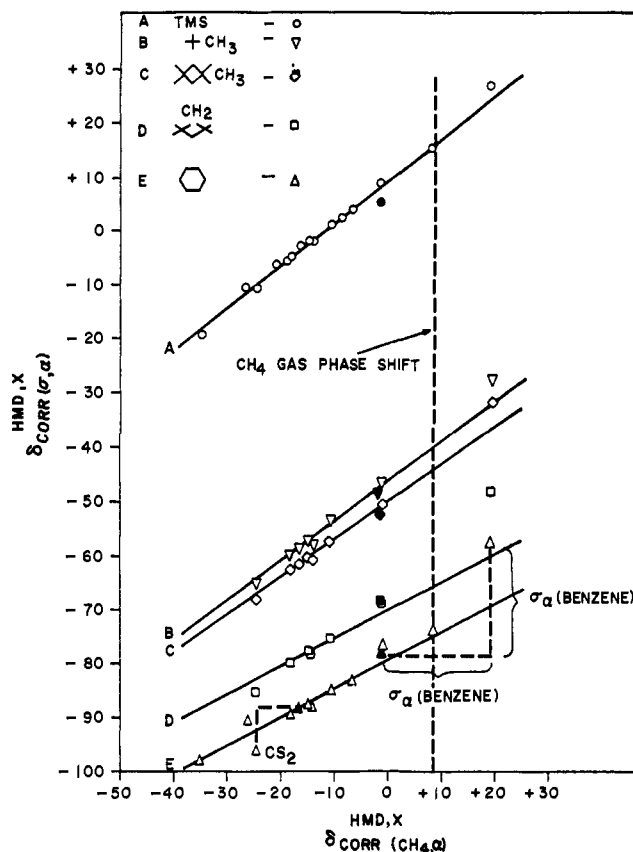


Figure 1. Chemical shift of nonpolar solutes *vs.* the chemical shift of methane in the same solvent.

tetramethylcyclobutane, -44 Hz; and for the methylene group of 1,1,3,3-tetramethylcyclobutane, -65.4 Hz.

To understand the nature of the slope we proceed as follows. For two solutes *i* and *j* dissolved in solvents α and β , we define the following quantities.

$$\begin{aligned} \Delta(i, \alpha) &= \delta_{\text{cor}}^{\text{HMD}, x}(i, \alpha) - \sigma_a(\alpha) = \delta_g^{\text{HMD}}(i) + \sigma_w(i, \alpha) \\ \Delta(j, \alpha) &= \delta_{\text{cor}}^{\text{HMD}, x}(j, \alpha) - \sigma_a(\alpha) = \delta_g^{\text{HMD}}(j) + \sigma_w(j, \alpha) \end{aligned} \quad (7)$$

$$\begin{aligned} \Delta(i, \beta) &= \delta_{\text{cor}}^{\text{HMD}, x}(i, \beta) - \sigma_a(\beta) = \delta_g^{\text{HMD}}(i) + \sigma_w(i, \beta) \\ \Delta(j, \beta) &= \delta_{\text{cor}}^{\text{HMD}, x}(j, \beta) - \sigma_a(\beta) = \delta_g^{\text{HMD}}(j) + \sigma_w(j, \beta) \end{aligned}$$

Upon examining these equations we contend that the slope *m* of each line shown in Figure 1 is given as

$$m = \frac{\Delta(j, \beta) - \Delta(j, \alpha)}{\Delta(i, \beta) - \Delta(i, \alpha)} \quad (8)$$

For solvents with zero anisotropy, $\Delta(i, \alpha) = \delta_{\text{cor}}^{\text{HMD}, x}(i, \alpha)$. Consequently

$$m = \frac{\delta_{\text{cor}}^{\text{HMD}, x}(j, \beta) - \delta_{\text{cor}}^{\text{HMD}, x}(j, \alpha)}{\delta_{\text{cor}}^{\text{HMD}, x}(i, \beta) - \delta_{\text{cor}}^{\text{HMD}, x}(i, \alpha)} \quad (9)$$

For this reason lines were drawn only through those points for which the solvent anisotropy is negligibly small (*i.e.*, only the halogenated solvents).

Data points for solutes in benzene and carbon disulfide are also shown in Figure 1. Notice that these points do not lie on the lines determined by the other solvents. This is dramatically illustrated in line E. In comparison to the other solvents the points for benzene lie to the opposite side of the gas-phase points. The gas-phase shift should be a limiting value since it represents the absence of solvent. These deviations can be understood by recognizing that both benzene and carbon disulfide have large solvent anisotropies. According to eq 7 the anisotropy contribution should be subtracted from the corrected shifts. (In reality, $\Delta(i,\alpha)$ vs. $\Delta(\text{CH}_4,\alpha)$ should be plotted instead of $\delta_{\text{cor}}^{\text{HMD},x}(i,\alpha)$ vs. $\delta_{\text{cor}}^{\text{HMD},x}(\text{CH}_4,\alpha)$ in order to yield a straight line.) For most solvents studied here, the anisotropy is negligibly small. Since the anisotropy effect for a solvent is independent of the solute, the same quantity must be subtracted from each coordinate axis. Subtracting approximately 21 Hz from each axis brings the benzene points onto the correct side of the gas-phase points and places these points closer to the lines (see solid black points). From the graph we estimate thus that the anisotropic shift for benzene is $+21 \pm 3$ Hz and for carbon disulfide is -9 ± 3 Hz. These values can be compared with the theoretical estimations of Schug,⁶ $+30.4$ Hz and -18.1 Hz for benzene and carbon disulfide, respectively. Homer⁷ estimates values of $+35$ Hz for benzene and -7 Hz for carbon disulfide by measuring the shift difference between TMS in benzene and in CCl_4 using an external standard, and then subtracting the van der Waals contribution by using the theoretical dispersion shift equations of Howard, Linder, and Emerson.⁸ Furthermore, from the graph we conclude that acetonitrile has a small anisotropic shift of approximately -3 Hz.

Inserting the right side of eq 6 into 7 we find that the slope is a function of van der Waals interaction terms, *i.e.*

$$m = \frac{\sigma_w(j,\beta) - \sigma_w(j,\alpha)}{\sigma_w(i,\beta) - \sigma_w(i,\alpha)} \quad (10)$$

If the van der Waals interaction can be expressed as a product function of solute and solvent parameters

$$\sigma_w(j,\beta) = \sigma_w(j)\sigma_w(\beta) \quad (11)$$

then eq 10 becomes

$$m = \frac{\sigma_w(j)}{\sigma_w(i)} \quad (12)$$

Thus the slope of the curve is a simple ratio of solute dispersion factors.

There is supporting evidence that the van der Waals term can be split into a product function. See, for example, the work of Bothner-By.⁹ Also, on the basis of a binary collision model, Rummens, Raynes, and Bernstein¹⁰ derived the following theoretical formula for the van der Waals shift of nonpolar solutes in nonpolar solvents.

(6) J. C. Schug, *J. Phys. Chem.*, **70**, 1816 (1966).

(7) J. Homer, *Tetrahedron*, **23**, 4065 (1967).

(8) B. B. Howard, B. Linder, and M. T. Emerson, *J. Chem. Phys.*, **36**, 485 (1962).

(9) A. A. Bothner-By, *J. Mol. Spectrosc.*, **5**, 52 (1960).

(10) F. H. A. Rummens, W. T. Raynes, and H. J. Bernstein, *J. Phys. Chem.*, **72**, 2111 (1968).

$$\sigma_w = K_6^g \frac{-\pi N B \alpha_2 I_2 H_6(y)}{V_2 r_0^3 y^4} S_6^g \quad (13)$$

Here K_6^g is a scale factor, B is a bond parameter, α_2 and I_2 are the polarizability and ionization potential of the perturbing solvent, V_2 is the molecular volume of the solvent molecule, $H_6(y)$ is a function of y tabulated by Buckingham and Pople¹¹ ($y = 2(\epsilon/kT)^{1/2}$), ϵ/k and r_0 are the force constants in the Lennard-Jones (6-12) potential, N is Avogadro's number, and S_6^g is a site factor to take into consideration the position of the hydrogens of interest in the solute molecule. If we make the following approximations, as suggested by Bernstein¹²

$$\begin{aligned} r_0 &= (r_1 r_2)^{1/2} \\ y &= (y_1 y_2)^{1/2} \end{aligned} \quad (14)$$

$$H_6(y) = \{[H_6(y_1)][H_6(y_2)]\}^{1/2}$$

where 1 refers to the solute and 2 refers to the solvent, eq 13 becomes

$$\sigma_w = \left[\frac{\pi N \alpha_2 I_2}{V_2 r_2^{3/2}} \left(\frac{H_6(y_2)}{y_2^4} \right)^{1/2} \right]_{\text{solvent}} \times \left[\frac{-B}{r_1^{3/2}} \left(\frac{H_6(y_1)}{y_1^4} \right)^{1/2} S_6^g \right]_{\text{solute}} \quad (15)$$

In this format we see that the van der Waals shift is a product of solute and solvent terms.

We can test the collision theory of Bernstein and coworkers¹⁰ by calculating the solute ratio of van der Waals terms as predicted by eq 15 and comparing this with the experimental slopes shown in Table III. It is interesting to note that although Bernstein's equation holds only for nonpolar solvents, points for polar and nonpolar solvents fall on the same lines as shown in Figure 1. The data used for this calculation were taken from the above paper. The radius of the solute molecule was set equal to the Lennard-Jones radius. The results are as follows.

$$\frac{\sigma_w(\text{TMS})}{\sigma_w(\text{CH}_4)} = 0.86 \text{ exptl, } 0.90 \text{ predicted}$$

$$\frac{\sigma_w(\text{neopentane})}{\sigma_w(\text{CH}_4)} = 0.83 \text{ exptl, } 0.73 \text{ predicted}$$

$$\frac{\sigma_w(\text{C}_6\text{H}_{12})}{\sigma_w(\text{CH}_4)} = 0.56 \text{ exptl, } 0.70 \text{ predicted}$$

The agreement is surprisingly good and lends credence to the collision theory of Bernstein and coworkers¹⁰ as well as to the empirical procedure described in the present paper.

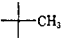

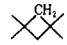
Referring to Figure 1, it is also possible to develop a relationship for the relative distances along the lines. First we define d_α as the distance along the line measured from the gas-phase point to the point of solvent α . Again considering only those solvents for which the anisotropy is negligible, and restricting the discussion to nonpolar solutes for which $\sigma_E \cong 0$, we readily deduce that

$$\frac{d_\alpha}{d_\beta} = \frac{\sigma_w(\alpha)}{\sigma_w(\beta)} \quad (16)$$

(11) A. D. Buckingham and J. A. Pople, *Trans. Faraday Soc.*, **51**, 1173 (1955).

(12) H. J. Bernstein, private communication.

Table IV. Distance d_α along the Various Solute-Solute Curves Measured from the Gas-Phase Points^a

Solvent	TMS				C ₆ H ₁₂
Acetone	12.3	12.8	12.1	11.7	11.8
CH ₂ Cl ₂	24.5	24.9	24.0	23.3	24.6
CH ₃ CN	28.2	29.3	28.6	27.7	28.8
CDCl ₃	29.1	29.9	29.0	28.1	29.5
CCl ₄	31.8	32.6	31.4	30.0	31.8
DMSO	33.9	33.9	33.0	31.9	33.4
CH ₃ I	34.7				
CH ₂ Br ₂	37.4				
CS ₂	42.7	43.0	41.5	40.0	42.4
CHBr ₃	44.1				38.0
CHI ₃	57.0				50.0
C ₆ H ₁₀	19.7				
C ₆ H ₁₂	21.9				

^a Values in Hz determined by distance formula between two points on a straight line.

a ratio of van der Waals factors concerning the solvents. Measured values for various d_α 's in units of Hz are presented in Table IV. We can again compare the collision model with the solvent ratios thus obtained. The results are

$$\frac{\sigma_w(\text{C}_6\text{H}_{10})}{\sigma_w(\text{CCl}_4)} = 0.62 \text{ exptl, } 0.71 \text{ predicted}$$

$$\frac{\sigma_w(\text{C}_6\text{H}_{12})}{\sigma_w(\text{CCl}_4)} = 0.69 \text{ exptl, } 0.69 \text{ predicted}$$

Again the agreement is surprisingly good considering the crudeness of the Lennard-Jones potential and the fact that these molecules are not really spherical.

Acknowledgment. This investigation was supported in part by the U. S. Army Research Office (Durham) under Contract No. DA-31-124-ARO-D-90.

The Effect of Solutes and Temperature on the Structure of Deuterium Oxide

O. D. Bonner

Contribution from the Department of Chemistry, University of South Carolina, Columbia, South Carolina 29208. Received December 17, 1969

Abstract: The spectrum of liquid D₂O has been observed over the range 1200–2000 $m\mu$ by a differential method in which D₂O at 25° is compared either with a salt solution at the same temperature or D₂O at an elevated temperature. Four combination bands have been observed, which may be identified with the same ones occurring in the vapor phase, and are apparently due to nonbonded D₂O. The band at 1893 $m\mu$ was used for quantitative studies, and solvation numbers have been calculated for several electrolytes. It appears that the ions are solvated to a greater extent than in H₂O but that the relative order of solvation is similar. The strength of the deuterium bond, as measured from the temperature dependence of the band intensity, is about 11% less than that of the hydrogen bond. Osmotic and activity coefficients are reported for solutions of tetramethylammonium chloride in D₂O, and a comparison of these data and those for alkali halides appearing in the literature seems to confirm the greater solvation of salts in D₂O.

The structure of water and of deuterium oxide is of considerable current interest. No bibliography of the literature on this subject will be attempted, but it may be noted that numerous experimental techniques have been used to measure the properties of the pure liquids and also a limited number of data are available for solutions of electrolytes and nonelectrolytes in the two solvents. A recent article by Holtzer and Emerson¹ points out some of the difficulties encountered in attempting to establish the relative degree of structure in the two liquids from a consideration of their physical properties. More extensive data for solutions in D₂O as a solvent appear to be needed for a comparison with those for H₂O solutions which are available in the literature.

Near-infrared spectra of water have been used in a recent paper² to determine the effect of solutes and temperature on its structure, and a logical extension of this work to the employment of these same techniques to D₂O and its solutions would appear to be profitable.

- (1) A. Holtzer and M. F. Emerson, *J. Phys. Chem.*, **73**, 261 (1969).
- (2) O. D. Bonner and G. B. Woolsey, *ibid.*, **72**, 899 (1968).

Experimental Section

Spectral Data. All spectra were recorded using a Cary Model 14M spectrophotometer. Corresponding bands of D₂O, both in the liquid and vapor state, are less intense than those of H₂O and it was necessary to use a special 0–0.2- $m\mu$ slide-wire in order to obtain a tenfold increase in sensitivity. Spectra were recorded for both pure D₂O and a saturated solution of LiCl in D₂O over the range 1200–1650 $m\mu$ using a 0.5-cm cell. Differential spectra (D₂O vs. various solutions) were recorded using the same techniques as previously reported² and employing matched 10-cm cells. Matched cells of 2-mm path length were employed for the differential spectra in the 1650–2000- $m\mu$ range. It was found that the bands due to "monomeric" D₂O which resulted from the differential measurements were quite similar to those found in H₂O but slightly broader.

Isopiestic Data. The osmotic and activity coefficients of tetramethylammonium chloride were determined by isopiestic comparison of its solutions with those of lithium chloride which served as a standard. Values of these coefficients of lithium chloride are tabulated by Kerwin.³

Results and Discussion

A. Vibrational Bands. The positions of the fundamental vibrational bands of D₂O vapor and their over-

- (3) R. E. Kerwin, Ph.D. Dissertation, University of Pittsburgh, 1964.